JOURNAL OF GUIDANCE, CONTROL, AND DYNAMICS
Vol. 33, No. 5, September–October 2010

New Solar Radiation Pressure Force Model for Navigation

Jay W. McMahon* and Daniel J. Scheeres†
University of Colorado, Boulder, Colorado 80309

DOI: 10.2514/1.48434

This paper presents a new force model for solar radiation pressure acting on a satellite. The model is based on a Fourier series representation of the satellite properties and the position of the sun with respect to the body. The perturbative effects on the satellite's orbit due to the solar radiation pressure are derived in full and subsequently averaged to determine the secular change in the orbit due to solar radiation pressure, as well as the short-period dynamics. The theory presented includes a methodology for analyzing the changes to the secular and short-period dynamics due to the spacecraft passing through the Earth's shadow. This preliminary study shows that for a spacecraft in a circular orbit with synchronous rotation, the secular effects of solar radiation can be described with only seven Fourier coefficients. The benefits of using this theory for navigation applications are discussed. Finally, an example based on the Gravity Recovery and Climate Experiment satellite illustrates the applicability of the theory presented.

I. Introduction

THERE are a wide variety of solar radiation pressure (SRP) models used for spacecraft missions. The most widely used, due to its simplicity, is the cannonball model [1]. This model treats the spacecraft as a flat plate that is pointed directly at the sun. While this can capture the basic effects of the SRP force, the model is insufficient for use in missions with more precise orbit accuracy requirements. For higher accuracy, spacecraft are modeled to varying degrees of accuracy, from the macromodels for The Ocean Topography Experiment Poseidon (TOPEX/Poseidon) [2] or Gravity Recovery and Climate Experiment (GRACE) [3] to finite element models for Global Positioning System (GPS) [4] or Ice, Cloud, and Land Elevation Satellite (ICESat) [5]. The former models use analytical expressions to derive the SRP force, while the latter use Monte Carlo ray-tracing methods, which simulate the path of each photon. Other models exist in the literature as well [6,7]; however, all of these models suffer from the same weakness for orbit determination in that these models are used based on ground-measured data of the spacecraft. Once the spacecraft enters the space environment, however, many of the assumptions that go into these models will change in an unpredictable fashion, which will change the accelerations caused by the solar radiation pressure. Because of the manner in which these models are developed and used, it is nearly impossible to separate how errors in model parameters impact the spacecraft's orbit. The most common method to improve the model solution is to apply an estimated correction factor to all parts of the spacecraft equally; however, this method cannot capture all possible model errors as it changes the accelerations in all directions proportionally.

A different type of model was developed independently by Springer et al. [8] and Bar-Sever [9] to model the SRP effect on the orbits of GPS satellites. These models were developed to be optimal models for the SRP effects on GPS satellites in terms of minimizing the residuals of the orbit fit. In other words, this model was developed purely by looking at the orbital effects of SRP with no real attention being paid to the physics of the interaction that is causing these effects.

The approach presented in this paper combines these two methodologies. A precise, physics-based model of the SRP induced accelerations is combined with a perturbative theory of the accelerations on the orbit to create a system that combines a physical a priori model with a mathematical form that is conducive to studying the orbital effects and estimating the effect of SRP on the orbit.

The new force model presented here, which is based on Fourier series analysis, has several features. First, the model is derived in a way that analytically accounts for the main physical processes by which the SRP interaction induces a force on the spacecraft. This model also allows for a variation in how precise or rough of a shape model for the satellite will be used. Second, this model is written as a spatially periodic function, which highlights how the solar radiation pressure interacts with the spacecraft's periodic orbit and rotation. While we base our Fourier series on the analytical model for the SRP interaction mentioned above, the process for deriving and using the series representation is not tied to this model so if a better physical model appears, it can be adopted into the same structure presented here for analyzing the orbital effects. Third, this model allows for a unique method for analyzing the effects of the Earth's shadow, which is not easily available with other models. Another main advantage of the application of this model is that the parameters of the model can be estimated from flight data, allowing the model to be updated more accurately than current models. Finally, the model is derived specifically so that the secular and short-period effects on the orbit can be separated, which is nearly impossible with many other models. This will allow for better predictions to be made for how SRP will affect a spacecraft's orbit over long times.

In this paper, the analysis in [10] is extended to investigate the modeling of solar radiation pressure and its perturbative effects for spacecraft orbits. A number of issues specific to the spacecraft problem are addressed, including modeling complicated attitude motion, modeling moving parts (e.g., solar panels) in the body frame, comparison with commonly used spacecraft SRP models, and changes in the orbital effects due to shadowing. The perturbative effects are inherently periodic due to the Fourier series representation of the force, and so averaging theory is applied to determine the secular changes in the orbit. The discussion in this paper is limited to spacecraft in circular orbits; however, the same approach is used for eccentric orbits and the results for the general case are presented in [10]. An immediate benefit is seen from the averaging theory for satellites that rotate synchronously in a circular orbit. In this case, only seven Fourier coefficients are needed to model the secular changes to a circular orbit.

This paper is organized as follows. First, the mathematical representation of the system is discussed. Second, the new force model is presented and discussed. Next, the orbit variational

Presented at the 2009 AIAA/AAS Astrodynamics Specialist Conference and Exhibit, Pittsburgh, PA, 10–13 August 2009; received 10 December 2009; revision received 14 June 2010; accepted for publication 15 June 2010.

*Graduate Research Assistant, Aerospace Engineering Sciences, 431 UCB.

†Richard Seabass Endowed Professor, Aerospace Engineering Sciences, 429 UCB.

equations are derived and applied specifically to circular orbits. The variational equations are averaged to show the short- and long-term effects of the solar radiation pressure. An example for a satellite based on GRACE is shown to illustrate the applicability of this work. The methodology being used to address Earth shadowing is included, followed by a discussion of the navigation applications and benefits of this work.

II. Coordinate Frame Definitions

To use the averaging theory shown in this paper to get a simple representation of the secular effects of solar radiation pressure on the spacecraft's orbit requires some assumption on the rotational motion of the spacecraft. In general, the theory requires the spacecraft's attitude motion to be periodic with the same period as the orbit. The body frame tracks this attitude motion in inertial space. This is a reasonable assumption for many spacecraft. For example, the GRACE spacecraft always keep a constant attitude with respect to Earth; the GPS spacecraft always keep one side pointed at Earth while executing a periodic yaw maneuver that has the same period as the orbit; gravity gradient spacecraft in circular orbits librate with respect to the local vertical, but the period of the libration is the same as the orbit period.

The inertial frame can be described by the unit vectors $\hat{\mathbf{X}}_I$, $\hat{\mathbf{Y}}_I$, and $\hat{\mathbf{Z}}_I$. This frame can be specified according to whichever convention is convenient. The heliocentric frame is defined by $\hat{\mathbf{X}}_H$, which is the unit vector pointing along the perihelion radius vector, $\hat{\mathbf{Z}}_H$, which is the unit vector pointing along the orbit angular momentum vector, and $\hat{\mathbf{Y}}_H$, which is the unit vector pointing along the perihelion velocity vector, which completes the triad.

The satellite orbit frame is defined in a manner similar to the heliocentric frame. The basis vectors are $\hat{\mathbf{e}}$, the unit vector along the eccentricity vector, which is in the direction of periapsis, $\hat{\mathbf{h}}$, the unit vector in the direction of the angular momentum, and $\hat{\mathbf{e}}_\perp$, which is in the direction of the velocity at periapsis and completes the triad. These vectors can be expressed with respect to the inertial frame by the classical orbital elements as

$$\hat{\mathbf{e}} = [\cos\bar{\omega}\cos\Omega - \sin\bar{\omega}\sin\Omega\cos i]\hat{\mathbf{X}}_I + [\cos\bar{\omega}\sin\Omega + \sin\bar{\omega}\cos\Omega\cos i]\hat{\mathbf{Y}}_I + \sin\bar{\omega}\sin i\hat{\mathbf{Z}}_I \tag{1}$$

$$\hat{\mathbf{e}}_\perp = -[\sin\bar{\omega}\cos\Omega + \cos\bar{\omega}\sin\Omega\cos i]\hat{\mathbf{X}}_I + [-\sin\bar{\omega}\sin\Omega + \cos\bar{\omega}\cos\Omega\cos i]\hat{\mathbf{Y}}_I + \cos\bar{\omega}\sin i\hat{\mathbf{Z}}_I \tag{2}$$

$$\hat{\mathbf{h}} = \sin\Omega\sin i\hat{\mathbf{X}}_I - \cos\Omega\sin i\hat{\mathbf{Y}}_I + \cos i\hat{\mathbf{Z}}_I \tag{3}$$

where i is the inclination, Ω is the right ascension of the ascending node, and $\bar{\omega}$ is the argument of periapsis of the satellite. Throughout this paper the notation above will be used, where a bold term is a vector, nonbold is the magnitude, and bold with a hat over it is a unit vector along the vector.

The rotating frame is defined with respect to the satellite orbit frame by a rotation of the mean anomaly angle about the angular momentum vector. Therefore, its basis vectors are $\hat{\mathbf{p}}$, $\hat{\mathbf{q}}$, and $\hat{\mathbf{h}}$. These vectors are defined by

$$\hat{\mathbf{p}} = \cos M\hat{\mathbf{e}} + \sin M\hat{\mathbf{e}}_\perp \tag{4}$$

$$\hat{\mathbf{q}} = -\sin M\hat{\mathbf{e}} + \cos M\hat{\mathbf{e}}_\perp \tag{5}$$

$$\hat{\mathbf{h}} = \hat{\mathbf{h}} \tag{6}$$

where M is the mean anomaly of the satellite in its orbit. The rotating frame is similar to the local-vertical/local-horizontal frame; in fact, the two are the same for circular orbits.

To map a vector quantity from the rotating frame to the orbit frame, the rotation matrix is

$$[\mathrm{OR}] = \begin{bmatrix} \cos(M) & -\sin(M) & 0 \\ \sin(M) & \cos(M) & 0 \\ 0 & 0 & 1 \end{bmatrix} \tag{7}$$

The location of the sun in the rotating frame, $\hat{\mathbf{u}}$, can be described as

$$\hat{\mathbf{u}} = \cos\delta_s\cos\lambda_s\hat{\mathbf{p}} + \cos\delta_s\sin\lambda_s\hat{\mathbf{q}} + \sin\delta_s\hat{\mathbf{h}} \tag{8}$$

where δ_s and λ_s are the solar latitude and longitude, respectively. These angles are defined in Fig. 1.

The solar longitude can be related to the mean anomaly of the orbit as

$$\lambda_s = \lambda_{s_0} - M \tag{9}$$

where λ_{s_0} is the longitude of the sun in the rotating frame at $M = 0$. This angle changes over the course of the year as the Earth moves in its orbit about the sun, the details of which are discussed in [10]. This relationship, combined with Eq. (8), tells us that for a fixed location on the heliocentric orbit, the sun's longitude precesses in a retrograde fashion as seen by the rotating frame due only to the frame's rotation. Therefore, for one orbit about the Earth, the sun makes one revolution in the rotating frame at a near constant latitude in the rotating frame.

The body frame is represented by the unit vectors $\hat{\mathbf{x}}_b, \hat{\mathbf{y}}_b, \hat{\mathbf{z}}_b$. There are two types of attitude motion that a spacecraft can have for the theory presented here to be useful. First, in the general case, all that is required in this paper is that the body-frame attitude is periodic with the orbit. Therefore, there will exist a mapping from the body frame to the rotating frame that depends on the mean anomaly M. An example of a satellite that fits in this general type of motion is the GPS satellites, which perform a yaw maneuver to keep the solar panels aligned with the sun while also keeping one face always pointed at the center of the Earth.

The second type of attitude motion is more specific and will be referred to as synchronous rotation. This means that the spacecraft's rotation axis is parallel to the angular momentum vector and that it rotates at a constant rate such that it completes one revolution per orbit. This assumption implies that for the circular orbits considered here, the spacecraft has one side always facing the Earth as it orbits. Mathematically, this has the following implications.

First, the spacecraft rotates only about $\hat{\mathbf{z}}_b$, which is assumed to be aligned with the orbit angular momentum vector:

$$\hat{\mathbf{z}}_b = \hat{\mathbf{h}} \tag{10}$$

Second, the satellite is assumed to rotate at a constant rate of one rotation per orbit. Therefore, we can write

$$\phi = nt + \phi_0 = M + \phi_0 \tag{11}$$

where ϕ is the rotation angle of the body frame (the angle between $\hat{\mathbf{e}}$ and $\hat{\mathbf{x}}_b$), n is the mean motion of the satellite's orbit, and ϕ_0 is a constant phase angle that describes the offset between $\hat{\mathbf{x}}_b$ and $\hat{\mathbf{y}}_b$ and $\hat{\mathbf{p}}$ and $\hat{\mathbf{q}}$. An example of a satellite in synchronous rotation is GRACE.

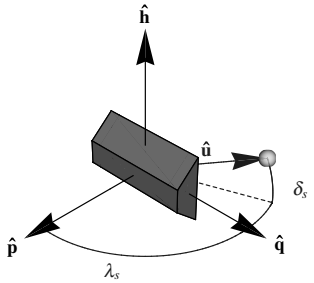

Fig. 1 Illustration of the rotating coordinate frame defining the solar longitude λ_s measured from $\hat{p}$ and the solar latitude δ_s measured from the $\hat{p} - \hat{q}$ plane. The rotating frame rotates about $\hat{h}$ in a positive sense; therefore, the sun will appear to rotate in a negative sense when viewed in this plane.

III. Solar Radiation Pressure Model

A functional expression for the force acting on the spacecraft due to the solar radiation pressure is derived here. This representation is derived in the spacecraft body frame, because the magnitude and direction of the force vector is intrinsically tied to body-fixed properties. Recall that the only assumption necessary is that the spacecraft's attitude motion repeats each orbit. This has the effect that the force vector will also repeat each orbit (for a given position of the Earth in its heliocentric orbit). This information can be used to map the force vector to the rotating frame, where the force is decomposed as a Fourier series over the mean anomaly. Finally, the acceleration will be related to the orbit frame in order to be used in the orbit variational equations.

The solar radiation force can be computed by summing the force imparted on each facet of the spacecraft as

$$\mathbf{F}_{\text{SRP}} = P(R)\sum_{i=1}^{N}\mathbf{f}_i(\hat{\mathbf{u}}) \tag{12}$$

where $P(R)$ is the solar radiation pressure at a given distance from the sun R, given to first order as

$$P(R) = \frac{G_1}{R^2} \tag{13}$$

where G_1 is the solar radiation force constant at 1 AU (astronomical unit) and is approximately equal to 1×10^{14} kg km/s^2, and the spacecraft–sun distance is assumed to vary with the true anomaly following Keplerian motion, which gives

$$R = \frac{a_s(1-e_s^2)}{1+e_s\cos\nu_s} \tag{14}$$

where a_s and e_s are the semimajor axis and eccentricity of the heliocentric orbit, and ν_s is the true anomaly of the Earth in its heliocentric orbit.

The interaction between the solar radiation pressure and a surface element of the body was derived by Scheeres [11] to be

$$\mathbf{f}_i = -[\{\rho_i s_i(2\hat{\mathbf{n}}_i\hat{\mathbf{n}}_i - \bar{\bar{U}}) + \bar{\bar{U}}\}\cdot\hat{\mathbf{u}}\,\hat{\mathbf{u}}\cdot\hat{\mathbf{n}}_i + a_{2i}\hat{\mathbf{n}}_i\hat{\mathbf{n}}_i\cdot\hat{\mathbf{u}}]H_i(\hat{\mathbf{u}})A_i \tag{15}$$

with

$$a_{2i} = B(1-s_i)\rho_i + (1-\rho_i)B \tag{16}$$

where i is the index for each surface of the satellite. Each surface has a normal unit vector $\hat{\mathbf{n}}_i$, a surface area A_i, and specular and diffuse reflectivity coefficients s_i and ρ_i, respectively. B is the Lambertian scattering coefficient of the surface (ideally equal to $2/3$), $\hat{\mathbf{u}}$ is the sun unit vector from the surface to the sun, $\bar{\bar{U}}$ is the identity dyad, and $H(\hat{\mathbf{u}})$ is the visibility function that equals 1 when the sun is above the horizon and 0 otherwise.

This model represents the physics of the SRP interacting with the surface and the force imparted considering specular and diffuse reflection, as well as assuming that all absorbed radiation is immediately reradiated diffusely. It should be noted here that if finite thermal inertia is being considered, this will result in a time delay affecting the second term of a_2, which represents the radiation that is absorbed and reradiated. This can be represented by having that term reradiated in a different direction (representing the normal vector's rotation during the time delay). Similarly, if not all of the absorbed radiation is reradiated, then an appropriate coefficient can be put here. Another effect that can be added to the given framework is that of self-shadowing. In this case, a slight modification to the definition of the piecewise function $H(\hat{\mathbf{u}})$ will allow for different periods of shadowing.

With this model we are able to compute the force acting on the body for any location of the sun with respect to the body. Given a specific spacecraft, the attitude motion can be used to determine the force vector over time, which can then be associated with the orbit time history.

It is generally assumed that the normal vector for a surface facet, $\hat{\mathbf{n}}_i$, will be constant in the body frame, as would be the case for both Laser Geodynamics Satellites (LAGEOS) and GRACE. However, many satellites have parts that will move in the body frame: for example, solar panels that track the sun (as is the case for GPS). If this motion follows the sun, it is straightforward to incorporate, as the normal vectors for these facets will always be equal to the sun position unit vector. In the more general case, when the motion is periodic with the orbit but not tracking the sun's movement, the time-varying force can still be computed for every location of the sun by taking into account the time-varying normal vectors for the moving parts. In either case, the following results are fully applicable.

This model for the SRP force is very similar to the macromodels built with geometric primitives such as those developed for GPS [12], GRACE [3], TOPEX/Poseidon [2], or ICESat [5]. If only one facet is kept in our model, we are effectively reproducing the cannonball model from LAGEOS [1]. By increasing the number of facets used in our model, the accuracy of the true shape and properties of the spacecraft can be retained similar to detailed ray-tracing models [4]. However, one difference between the highly detailed ray-tracing models is that our model does not account for secondary impact of photons due to the reflected light impacting another part of the spacecraft. Using ray-tracing models to reproduce this effect is a numerical process that requires significant computational power, which does not coincide with the goals of our analytical model. The main benefits of our model, however, do not come from the a priori model, but rather from the Fourier analysis we apply to this force in the rotating frame. This analysis allows us to move from a model of the SRP physics to an observation of how this force can affect the orbit. By estimating the coefficients based on the changes to the orbit, the model can account for unmodeled processes (such as secondary photon impact), as well as differences between the physical properties used to derive the a priori coefficients and those actually on the spacecraft.

Equations (12) and (15) are vector equations and can be defined in any frame. In general, it will usually be easiest to compute the force in the body frame due to the presence of the normal vectors for each surface facet. In any case, however, the time history of the attitude can be used to express the solar radiation force over the orbit in the rotating frame. This allows us to decompose the force vector as a Fourier series over the solar longitude:

$$\mathbf{F}_{\text{SRP}} = P(R)\sum_{n=0}^{\infty}[\mathbf{A}_n(\delta_s)\cos(n\lambda_s) + \mathbf{B}_n(\delta_s)\sin(n\lambda_s)] \tag{17}$$

where the Fourier coefficients are derived as

$$\mathbf{A}_0 = \frac{1}{2\pi}\int_0^{2\pi}\frac{\mathbf{F}_{\text{SRP}}}{P(R)}\,\mathrm{d}\lambda_s \tag{18}$$

$$\mathbf{A}_n = \frac{1}{\pi}\int_0^{2\pi}\frac{\mathbf{F}_{\text{SRP}}}{P(R)}\cos(n\lambda_s)\,\mathrm{d}\lambda_s \tag{19}$$

$$\mathbf{B}_n = \frac{1}{\pi}\int_0^{2\pi}\frac{\mathbf{F}_{\text{SRP}}}{P(R)}\sin(n\lambda_s)\,\mathrm{d}\lambda_s \tag{20}$$

In general, the solar radiation force is also a function of the solar latitude, δ_s, as shown in Eq. (17). However, this dependence will be suppressed from here forward. For a given number of orbits of the spacecraft about the Earth, the solar latitude is effectively constant, as the position on the heliocentric orbit changes much more slowly than the spacecraft's orbit rate. Therefore, the analysis will first be conducted over one spacecraft orbit. Following this, the dependence on the solar latitude will be reintroduced when the analysis for the effects over a heliocentric orbit is conducted.

Using Eq. (9), the Fourier series can be represented as a function of the mean anomaly as

$$\mathbf{F}_{\text{SRP}} = P(R)\sum_{n=0}^{\infty}[\mathbf{A}'_n\cos(nM) + \mathbf{B}'_n\sin(nM)] \tag{21}$$

where the generalized Fourier coefficients are

$$\mathbf{A}'_n = \cos(n\lambda_{s_0})\mathbf{A}_n + \sin(n\lambda_{s_0})\mathbf{B}_n \tag{22}$$

$$\mathbf{B}'_n = \cos(n\lambda_{s_0})\mathbf{B}_n - \sin(n\lambda_{s_0})\mathbf{A}_n \tag{23}$$

These generalized Fourier coefficients take into account the current location of Earth in its heliocentric orbit through the presence of λ_{s0}.

It is worth noting that for the synchronous rotation case, we can derive a set of Fourier coefficients in the body frame in a manner similar to the generalized coefficients in Eqs. (22) and (23). In this case, the relationship in Eq. (11) can be used with Eq. (9) to relate λ_s to ϕ as

$$\lambda_s = \lambda_{s_0} + \phi_0 - \phi \tag{24}$$

Using this relationship, the SRP force can be written as

$$\mathbf{F}_{\text{SRP}} = P(R)\sum_{n=0}^{\infty}[\mathbf{A}'_{B,n}\cos(n\phi) + \mathbf{B}'_{B,n}\sin(n\phi)] \tag{25}$$

where the synchronous body Fourier coefficients are defined as

$$\mathbf{A}'_{B,n} = \cos(n(\lambda_{s_0} + \phi_0))\mathbf{A}_n + \sin(n(\lambda_{s_0} + \phi_0))\mathbf{B}_n \tag{26}$$

$$\mathbf{B}'_{B,n} = \cos(n(\lambda_{s_0} + \phi_0))\mathbf{B}_n - \sin(n(\lambda_{s_0} + \phi_0))\mathbf{A}_n \tag{27}$$

It is important to recall that the Fourier coefficients are defined in the rotating frame by their derivation. However, in order to investigate the effects of this force on the satellite's orbit, they need to be mapped to the orbit frame. This can be done by applying the rotation matrix given in Eq. (7), so the Fourier series representation of the SRP force will become

$${}^{O}\mathbf{F}_{\text{SRP}} = P(R)\sum_{n=0}^{\infty}\{[\text{OR}]\mathbf{A}'_n\cos(nM) + [\text{OR}]\mathbf{B}'_n\sin(nM)\} \tag{28}$$

where the superscript O denotes the fact that this vector is expressed in orbit frame coordinates.

Finally, the acceleration caused by the solar radiation pressure on the satellite is represented in the orbit frame by

$${}^{O}\mathbf{a}_{\text{SRP}} = \frac{P(R)}{m}\sum_{n=0}^{\infty}\{[\text{OR}]\mathbf{A}'_n\cos(nM) + [\text{OR}]\mathbf{B}'_n\sin(nM)\} \tag{29}$$

where m is the mass of the satellite.

While we use Eq. (15) to determine the force imparted on a spacecraft by SRP, this is not necessary. Technically, any method can be used to determine the time history of the SRP force due to a spacecraft's periodic attitude motion. This can then be mapped to the rotating frame and decomposed as a Fourier series as shown here, which will allow all of the following analysis to hold.

IV. Orbital Effects of Solar Radiation Pressure

The focus of this research is not only the new method for expressing the solar radiation pressure model discussed in Sec. III, but also the predictions of the changes to the orbit based on this model. These predictions are studied in this section. Section IV.A outlines the derivation for the variational equations for the orbit. Section IV.B and IV.C give derivations for the secular and periodic effects of the SRP model, respectively. Finally, Sec. IV.D discusses how the effects can be averaged over a year to determine the long-term secular effects of SRP.

A. Orbit Variational Equations

General variational equations for the orbit energy $\mathcal{E}$, angular momentum $\mathbf{h}$, and the eccentricity vector $\mathbf{e}$ are derived to describe the effect of solar radiation pressure on the satellite's orbit. While this set is not the most common set of elements used to describe an orbit, it has nice properties in that these quantities can be used to define any other orbital elements, and the variation of these quantities can be described for all orbits, including circular and equatorial. The general variational equations were derived in [10] to be

$$\dot{\mathcal{E}} = \frac{h}{a(1-e^2)}[(-\sin(\nu))\hat{\mathbf{e}} + (e+\cos(\nu))\hat{\mathbf{e}}_\perp]\cdot\mathbf{a} \tag{30}$$

$$\dot{\mathbf{h}} = \frac{a(1-e^2)}{1+e\cos(\nu)}[\cos(\nu)\hat{\mathbf{e}} + \sin(\nu)\hat{\mathbf{e}}_\perp]\cdot\tilde{\mathbf{a}} \tag{31}$$

$$\begin{aligned}\dot{\mathbf{e}} = \frac{1}{\mu}\{&-\tilde{\mathbf{h}} + \frac{h}{1+e\cos(\nu)}[-\cos(\nu)\sin(\nu)\hat{\mathbf{e}}\,\hat{\mathbf{e}} - \sin^2(\nu)\hat{\mathbf{e}}_\perp\hat{\mathbf{e}}\\ &+ \cos(\nu)[e+\cos(\nu)]\hat{\mathbf{e}}\hat{\mathbf{e}}_\perp + \sin(\nu)[e+\cos(\nu)]\hat{\mathbf{e}}_\perp\hat{\mathbf{e}}_\perp\\ &- e\sin(\nu)\bar{\bar{U}}]\}\cdot\mathbf{a}\end{aligned} \tag{32}$$

where μ is the gravitational parameter of the Earth, e is the eccentricity, a is the semimajor axis, h is the angular momentum magnitude, ν is the true anomaly, and $\mathbf{a}$ is the disturbing acceleration acting on the satellite. The tilde operator over a vector represents the cross-product dyad of the associated vector given by

$$\tilde{\mathbf{a}} = \begin{bmatrix} 0 & -\mathbf{a}(3) & \mathbf{a}(2) \\ \mathbf{a}(3) & 0 & -\mathbf{a}(1) \\ -\mathbf{a}(2) & \mathbf{a}(1) & 0 \end{bmatrix} \tag{33}$$

At this point, the expression for the solar radiation pressure acceleration from Eq. (29) can be inserted into Eqs. (30–32) to obtain explicit expressions for the effect the solar radiation pressure has on the satellite's orbit. To make the algebra easy to see, we rewrite the rotation matrix from Eq. (7) in dyadic notation:

$$\begin{aligned}[\text{OR}] = &\cos(M)\hat{\mathbf{e}}\,\hat{\mathbf{p}} - \sin(M)\hat{\mathbf{e}}\,\hat{\mathbf{q}} + \sin(M)\hat{\mathbf{e}}_\perp\hat{\mathbf{p}}\\ &+ \cos(M)\hat{\mathbf{e}}_\perp\hat{\mathbf{q}} + \hat{\mathbf{h}}\,\hat{\mathbf{h}}\end{aligned} \tag{34}$$

Using this result, the variational equations due to the solar radiation pressure acceleration are

$$\begin{aligned}\dot{\mathcal{E}} = \frac{P(R)}{m}\frac{h}{a(1-e^2)}&[-\sin(\nu)(\cos(M)\hat{\mathbf{p}} - \sin(M)\hat{\mathbf{q}})\\ &+ (e+\cos(\nu))(\sin(M)\hat{\mathbf{p}} + \cos(M)\hat{\mathbf{q}})]\\ &\cdot\sum_{n=0}^{\infty}[\mathbf{A}'_n\cos(nM) + \mathbf{B}'_n\sin(nM)]\end{aligned} \tag{35}$$

$$\begin{aligned}\dot{\mathbf{h}} = \frac{P(R)}{m}\frac{a(1-e^2)}{1+e\cos(\nu)}&[\cos(\nu)[\sin(M)\hat{\mathbf{h}}\,\hat{\mathbf{p}} + \cos(M)\hat{\mathbf{h}}\,\hat{\mathbf{q}} - \hat{\mathbf{e}}_\perp\hat{\mathbf{h}}]\\ &+ \sin(\nu)[-\cos(M)\hat{\mathbf{h}}\,\hat{\mathbf{p}} + \sin(M)\hat{\mathbf{h}}\,\hat{\mathbf{q}} + \hat{\mathbf{e}}\,\hat{\mathbf{h}}]]\\ &\cdot\sum_{n=0}^{\infty}[\mathbf{A}'_n\cos(nM) + \mathbf{B}'_n\sin(nM)]\end{aligned} \tag{36}$$

$$\begin{aligned}\dot{\mathbf{e}} = \frac{P(R)}{m}\frac{h}{\mu}\{&-(\cos(M)\hat{\mathbf{e}}_\perp\hat{\mathbf{p}} - \sin(M)\hat{\mathbf{e}}_\perp\hat{\mathbf{q}}\\ &- \sin(M)\hat{\mathbf{e}}\,\hat{\mathbf{p}} - \cos(M)\hat{\mathbf{e}}\,\hat{\mathbf{q}})\\ &+ \frac{1}{1+e\cos(\nu)}[-\cos(\nu)\sin(\nu)(\cos(M)\hat{\mathbf{e}}\,\hat{\mathbf{p}} - \sin(M)\hat{\mathbf{e}}\,\hat{\mathbf{q}})\\ &- \sin^2(\nu)(\cos(M)\hat{\mathbf{e}}_\perp\hat{\mathbf{p}} - \sin(M)\hat{\mathbf{e}}_\perp\hat{\mathbf{q}})\\ &+ \cos(\nu)[e+\cos(\nu)](\sin(M)\hat{\mathbf{e}}\,\hat{\mathbf{p}} + \cos(M)\hat{\mathbf{e}}\,\hat{\mathbf{q}})\\ &+ \sin(\nu)[e+\cos(\nu)](\sin(M)\hat{\mathbf{e}}_\perp\hat{\mathbf{p}} + \cos(M)\hat{\mathbf{e}}_\perp\hat{\mathbf{q}})\\ &- e\sin(\nu)(\cos(M)\hat{\mathbf{e}}\,\hat{\mathbf{p}} - \sin(M)\hat{\mathbf{e}}\,\hat{\mathbf{q}} + \sin(M)\hat{\mathbf{e}}_\perp\hat{\mathbf{p}}\\ &+ \cos(M)\hat{\mathbf{e}}_\perp\hat{\mathbf{q}} + \hat{\mathbf{h}}\,\hat{\mathbf{h}})]\}\cdot\sum_{n=0}^{\infty}[\mathbf{A}'_n\cos(nM) + \mathbf{B}'_n\sin(nM)]\end{aligned} \tag{37}$$

For a circular orbit, the eccentricity is zero, and therefore $\hat{\mathbf{e}}$ and ν are undefined. To resolve this, an arbitrary vector $\hat{\mathbf{a}}$ in the orbital plane is chosen, and ν is replaced with θ, which is just the angle between the current satellite position vector and $\hat{\mathbf{a}}$, measured in the positive direction about the angular momentum vector. Given this, we can state

$$\nu = M = \theta \tag{38}$$

and therefore

$$\mathrm{d}M = \mathrm{d}\theta \tag{39}$$

A third unit vector, $\hat{\mathbf{b}} = \hat{\mathbf{h}} \times \hat{\mathbf{a}}$, completes the basis set $\{\hat{\mathbf{a}}, \hat{\mathbf{b}}, \hat{\mathbf{h}}\}$.

Using these definitions, and recognizing that for a circular orbit $e = 0$, Eqs. (35–37) simplify to

$$\dot{\mathcal{E}} = \frac{P(R)}{m}\frac{h}{a}\hat{\mathbf{q}} \cdot \sum_{n=0}^{\infty}[\mathbf{A}'_n \cos(n\theta) + \mathbf{B}'_n \sin(n\theta)] \tag{40}$$

$$\dot{\mathbf{h}} = \frac{P(R)}{m} a[\sin(\theta)\hat{\mathbf{a}}\,\hat{\mathbf{h}} - \cos(\theta)\hat{\mathbf{b}}\,\hat{\mathbf{h}} + \hat{\mathbf{h}}\,\hat{\mathbf{q}}] \cdot \sum_{n=0}^{\infty}[\mathbf{A}'_n \cos(n\theta) + \mathbf{B}'_n \sin(n\theta)] \tag{41}$$

$$\dot{\mathbf{e}} = \frac{P(R)}{m}\frac{h}{\mu}[\sin(\theta)\hat{\mathbf{a}}\,\hat{\mathbf{p}} + 2\cos(\theta)\hat{\mathbf{a}}\,\hat{\mathbf{q}} - \cos(\theta)\hat{\mathbf{b}}\,\hat{\mathbf{p}} + 2\sin(\theta)\hat{\mathbf{b}}\,\hat{\mathbf{q}}] \cdot \sum_{n=0}^{\infty}[\mathbf{A}'_n \cos(n\theta) + \mathbf{B}'_n \sin(n\theta)] \tag{42}$$

Note that the change in the angular momentum vector has components in all three orbital frame directions, while the change in eccentricity is confined to the orbital plane. This inconsistency appears due to the circular assumptions we have made. Since for the circular case the magnitude of the eccentricity vector is zero, when the eccentricity vector does appear due to the SRP acceleration, it must appear in the orbital plane.

B. Secular Dynamics

Equations (40–42) give the instantaneous effect solar radiation pressure has on the orbit of a satellite in terms of the Fourier coefficient model. To determine any secular changes in the orbit, we can average these equations over the orbit as

$$\bar{\dot{\mathcal{E}}} = \frac{1}{2\pi}\int_0^{2\pi} \dot{\mathcal{E}}\,\mathrm{d}M \tag{43}$$

$$\bar{\dot{\mathbf{h}}} = \frac{1}{2\pi}\int_0^{2\pi} \dot{\mathbf{h}}\,\mathrm{d}M \tag{44}$$

$$\bar{\dot{\mathbf{e}}} = \frac{1}{2\pi}\int_0^{2\pi} \dot{\mathbf{e}}\,\mathrm{d}M \tag{45}$$

Carrying out the averaging (equivalently with respect to θ for the circular case) using the orthogonality conditions for trigonometric functions, the result is

$$\bar{\dot{\mathcal{E}}} = \frac{P(R)}{m}\frac{h}{a}\hat{\mathbf{q}} \cdot \mathbf{A}'_0 \tag{46}$$

$$\bar{\dot{\mathbf{h}}} = \frac{P(R)}{m}\frac{a}{2}[\hat{\mathbf{a}}\,\hat{\mathbf{h}} \cdot \mathbf{B}'_1 - \hat{\mathbf{b}}\,\hat{\mathbf{h}} \cdot \mathbf{A}'_1 + 2\hat{\mathbf{h}}\,\hat{\mathbf{q}} \cdot \mathbf{A}'_0] \tag{47}$$

$$\bar{\dot{\mathbf{e}}} = \frac{P(R)}{m}\frac{h}{2\mu}[\hat{\mathbf{a}}\,\hat{\mathbf{p}} \cdot \mathbf{B}'_1 + 2\hat{\mathbf{a}}\,\hat{\mathbf{q}} \cdot \mathbf{A}'_1 - \hat{\mathbf{b}}\,\hat{\mathbf{p}} \cdot \mathbf{A}'_1 + 2\hat{\mathbf{b}}\,\hat{\mathbf{q}} \cdot \mathbf{B}'_1] \tag{48}$$

Therefore, for the circular case, we can determine the secular variation of the orbital energy, angular momentum, and the eccentricity vector, with only the first three vector quantities of the Fourier series of the solar radiation force. Actually, we do not even need the full vector of the constant term; we need only the second component, $\mathbf{A}'_{0,2}$, for a total of seven components.

If we are concerned with a synchronously rotating spacecraft, then the same averaging analysis can be carried out with the body-frame Fourier coefficients to get

$$\bar{\dot{\mathcal{E}}} = \frac{P(R)}{m}\frac{h}{a}\hat{\mathbf{y}}_b \cdot \mathbf{A}'_{B,0} \tag{49}$$

$$\bar{\dot{\mathbf{h}}} = \frac{P(R)}{m}\frac{a}{2}[\hat{\mathbf{a}}\hat{\mathbf{z}}_b \cdot \mathbf{B}'_{B,1} - \hat{\mathbf{b}}\hat{\mathbf{z}}_b \cdot \mathbf{A}'_{B,1} + 2\hat{\mathbf{h}}\hat{\mathbf{y}}_b \cdot \mathbf{A}'_{B,0}] \tag{50}$$

$$\bar{\dot{\mathbf{e}}} = \frac{P(R)}{m}\frac{h}{2\mu}[\hat{\mathbf{a}}\hat{\mathbf{x}}_b \cdot \mathbf{B}'_{B,1} + 2\hat{\mathbf{a}}\hat{\mathbf{y}}_b \cdot \mathbf{A}'_{B,1} - \hat{\mathbf{b}}\hat{\mathbf{x}}_b \cdot \mathbf{A}'_{B,1} + 2\hat{\mathbf{b}}\hat{\mathbf{y}}_b \cdot \mathbf{B}'_{B,1}] \tag{51}$$

These results are exactly equivalent to those in Eqs. (46–48), as the Fourier coefficients were adjusted in step with the phase angle rotation that defines the difference between the rotating frame and the body frame for the synchronous case. The interesting result is that for the synchronous case, we can determine the secular change in the orbit directly from the Fourier coefficients based on the body without having to go through the rotating frame. This is possible because in the synchronous case, the body and rotating frames are a simple constant rotation apart at all times.

It is interesting to note that the development of the secular equations only required that the disturbing acceleration is periodic with the orbit. This implies that the secular equations would hold for any periodic disturbing acceleration and not only for solar radiation pressure. For a different disturbing acceleration the form would be the same, and the secular rates would depend on the same frequency terms from the new acceleration's Fourier decomposition.

C. Short-Period Dynamics

The focus of this research is to determine the secular change in a spacecraft's orbit due to SRP. However, there are two reasons we are still interested in the short-period dynamics. First, knowledge of the short-period dynamics will allow us to put bounds around the secularly changing orbit elements that will encompass the total variation of those elements. Second, when starting an integration of the mean orbit elements, it will often be the case that the current osculating element values will not be the same as the current mean element values. Using the short-period dynamics, we can determine the appropriate correction for mean element's initial conditions [13].

The value of an orbital element can be expressed at any time as a sum of the initial conditions oe_0, the secular term $\dot{\overline{\mathrm{oe}}}$, and the periodic terms oe_p as

$$\mathrm{oe}\,(t) = \mathrm{oe}_0 + \dot{\overline{\mathrm{oe}}}t + \mathrm{oe}_p \tag{52}$$

The average value of the orbital element over one orbit is then given by

$$\overline{\mathrm{oe}} = \mathrm{oe}_0 + \dot{\overline{\mathrm{oe}}}\frac{P}{2} + \overline{\mathrm{oe}}_p \tag{53}$$

where P is the orbit period. In the current development, oe_0 is a given, and we have determined $\dot{\overline{\mathrm{oe}}}$ in Eqs. (46–48). We will now determine $\overline{\mathrm{oe}}_p$.

The time derivative of Eq. (52) is rearranged to give a differential equation for the periodic term as

$$\dot{\mathrm{oe}}_p = f(\mathbf{x}, t) - \dot{\overline{\mathrm{oe}}}(\mathbf{x}) \tag{54}$$

where $f(\mathbf{x}, t)$ is the full dynamics for the orbital element represented in Eqs. (40–42), and $\mathbf{x}$ represents the vector of orbital elements.

Integrating this result over time gives the periodic term at a given time as

$$\mathrm{oe}_p(t) = \int_0^t f(\mathbf{x}_0, \tau)\,\mathrm{d}\tau - \dot{\overline{\mathrm{oe}}}(\mathbf{x}_0)t \tag{55}$$

Note that the secular rate is evaluated at the initial conditions $\mathbf{x}_0$. This is assumed valid because the higher-order effects of the change of the orbital elements over one period should be very small, assuming $t \leq P$.

After a change of variables from time to mean anomaly, the periodic term at a given point in the orbit is determined by

$$\mathrm{oe}_p(M) = \int_{M_0}^{M} \sqrt{\frac{a^3}{\mu}} f(\mathbf{x}_0, M')\,\mathrm{d}M' - (M - M_0)\sqrt{\frac{a^3}{\mu}}\dot{\overline{\mathrm{oe}}}(\mathbf{x}_0) \tag{56}$$

The periodic component for each orbital element can be determined, the derivation of which can be found in [10]. For example, for the orbit energy the periodic term is expressed as

$$\begin{aligned}\mathcal{E}_p = {} & \frac{P(R)}{m}\frac{h}{a}\sqrt{\frac{a^3}{\mu}}\hat{\mathbf{q}}\cdot\{\mathbf{A}_0'(M - M_0) + \sum_{n=1}^{\infty}\frac{1}{n}[\mathbf{A}_n'\sin(nM) \\ & - \mathbf{B}_n'\cos(nM) - \mathbf{A}_n'\sin(nM_0) + \mathbf{B}_n'\cos(nM_0)]\} \\ & - (M - M_0)\sqrt{\frac{a^3}{\mu}}\dot{\bar{\mathcal{E}}}(\mathbf{x}_0)\end{aligned} \tag{57}$$

The maximum and minimum over an orbit can be determined by varying M from 0 to 2π, and these values can be used to place upper and lower bounds on the mean values of the orbital elements to encompass the total variation.

To determine the average value of the periodic terms, we average the Eq. (56) over one orbit to get

$$\begin{aligned}\overline{\mathrm{oe}}_p = {} & \frac{1}{2\pi}\int_0^{2\pi}\mathrm{oe}_p\,\mathrm{d}M = \frac{1}{2\pi}\int_0^{2\pi}\left[\int_{M_0}^{M}\sqrt{\frac{a^3}{\mu}}f(\mathbf{x}_0, M')\,\mathrm{d}M'\right]\mathrm{d}M \\ & - (\pi - M_0)\sqrt{\frac{a^3}{\mu}}\dot{\overline{\mathrm{oe}}}(\mathbf{x}_0)\end{aligned} \tag{58}$$

This allows us to evaluate the initial condition for the averaged value of the orbital element to be

$$\dot{\overline{\mathrm{oe}}}(0) = \mathrm{oe}_0 + \dot{\overline{\mathrm{oe}}}_p \tag{59}$$

Recall that for the circular case under discussion here, $\theta = M$, and therefore this substitution can be made in Eqs. (40–42) before inserting them into Eq. (58). The averages of the periodic terms for each orbital element has been evaluated with $M_0 = 0$, and the resulting equations for the initial offsets are shown to be

$$\bar{\mathcal{E}}_p = \frac{P(R)}{m}\frac{h}{a}\sqrt{\frac{a^3}{\mu}}\hat{\mathbf{q}}\cdot\sum_{n=1}^{\infty}\left[\frac{1}{n}\mathbf{B}_n'\right] \tag{60}$$

$$\bar{\mathbf{h}}_{p1} = \frac{P(R)}{m}a\sqrt{\frac{a^3}{\mu}}\hat{\mathbf{a}}\,\hat{\mathbf{h}}\cdot\left\{\mathbf{A}_0' + \frac{1}{4}\mathbf{A}_1' + \sum_{n=2}^{\infty}\left[\frac{-\mathbf{A}_n'}{(n-1)(n+1)}\right]\right\} \tag{61}$$

$$\bar{\mathbf{h}}_{p2} = \frac{P(R)}{m}a\sqrt{\frac{a^3}{\mu}}\hat{\mathbf{b}}\,\hat{\mathbf{h}}\cdot\left\{-\frac{1}{4}\mathbf{B}_1' + \sum_{n=2}^{\infty}\left[\frac{-n\mathbf{B}_n'}{(n-1)(n+1)}\right]\right\} \tag{62}$$

$$\bar{\mathbf{h}}_{p3} = \frac{P(R)}{m}a\sqrt{\frac{a^3}{\mu}}\hat{\mathbf{h}}\,\hat{\mathbf{q}}\cdot\left[\sum_{n=1}^{\infty}\frac{1}{n}\mathbf{B}_n'\right] \tag{63}$$

$$\begin{aligned}\bar{\mathbf{e}}_{p1} = {} & \frac{P(R)}{m}\frac{h}{\mu}\sqrt{\frac{a^3}{\mu}}\left\{\hat{\mathbf{a}}\,\hat{\mathbf{p}}\cdot\left\{\mathbf{A}_0' + \frac{1}{4}\mathbf{A}_1' + \sum_{n=2}^{\infty}\left[\frac{-\mathbf{A}_n'}{(n-1)(n+1)}\right]\right\}\right. \\ & \left. + \hat{\mathbf{a}}\,\hat{\mathbf{q}}\cdot\left\{\frac{1}{2}\mathbf{B}_1' + \sum_{n=2}^{\infty}\left[\frac{2n\mathbf{B}_n'}{(n-1)(n+1)}\right]\right\}\right\}\end{aligned} \tag{64}$$

$$\begin{aligned}\bar{\mathbf{e}}_{p2} = {} & \frac{P(R)}{m}\frac{h}{\mu}\sqrt{\frac{a^3}{\mu}}\left\{\hat{\mathbf{b}}\,\hat{\mathbf{p}}\cdot\left\{-\frac{1}{4}\mathbf{B}_1' + \sum_{n=2}^{\infty}\left[\frac{-n\mathbf{B}_n'}{(n-1)(n+1)}\right]\right\}\right. \\ & \left. + \hat{\mathbf{b}}\,\hat{\mathbf{q}}\cdot\left\{2\mathbf{A}_0' + \frac{1}{2}\mathbf{A}_1' + \sum_{n=2}^{\infty}\left[\frac{-2\mathbf{A}_n'}{(n-1)(n+1)}\right]\right\}\right\}\end{aligned} \tag{65}$$

$$\bar{\mathbf{e}}_{p3} = 0 \tag{66}$$

The preceding equations show that the short-period dynamics depend on terms of all orders from the Fourier series expression of the SRP acceleration. This clearly demonstrates the difference between the secular dynamics, which depend on only seven coefficients and the short-period dynamics.

D. Year-Averaged Secular Effects

Up to this point, the inclination of the satellite orbit with respect to the sun has been ignored. However, the next step to take is to average the effects of the solar radiation on the satellite orbit over one year. Following the method set out in [11], the yearly average can be determined by first recognizing that for each of our orbital elements, the year-averaged secular rate equations can be written as

$$\dot{\bar{x}} = P(R)f(x, \nu_s') \tag{67}$$

where $\nu_s' = \bar{\omega}_s + \nu_s$, and $\bar{\omega}_s$ is the argument of perihelion. To average over one solar orbit, we take

$$\dot{\bar{x}} = \frac{1}{2\pi}\int_0^{2\pi} P(R)f(x, \nu_s')\,\mathrm{d}M \tag{68}$$

but the classical result $\mathrm{d}M = R^2/a_s^2\sqrt{1 - e_s^2}\,\mathrm{d}\nu_s'$ can be substituted, which results in

$$\dot{\bar{x}} = \frac{1}{2\pi}\frac{G_1}{a_s^2\sqrt{1 - e_s^2}}\int_0^{2\pi} f(x, \nu_s')\,\mathrm{d}\nu_s' \tag{69}$$

The averaged value for energy is

$$\dot{\bar{\mathcal{E}}} = \frac{G_1}{a_s^2\sqrt{1 - e_s^2}}\frac{h}{ma}[\bar{A}_0(2)] \tag{70}$$

The averaged values for angular momentum and eccentricity rates over a solar orbit are

$$\begin{aligned}\dot{\bar{\mathbf{h}}} = {} & \frac{G_1}{a_s^2\sqrt{1 - e_s^2}}\frac{a}{2m}[-\hat{\mathbf{a}}\,\hat{\mathbf{h}}[\bar{\mathbf{B}}_1\sin(\Omega_{s_0}) + \bar{\mathbf{A}}_1\cos(\Omega_{s_0})] \\ & + \hat{\mathbf{b}}\,\hat{\mathbf{h}}[\bar{\mathbf{A}}_1\sin(\Omega_{s_0}) + \bar{\mathbf{B}}_1\sin(\Omega_{s_0})] + 2\hat{\mathbf{h}}\,\hat{\mathbf{q}}\,\bar{\mathbf{A}}_0]\end{aligned} \tag{71}$$

$$\begin{aligned}\dot{\bar{\mathbf{e}}} = {} & \frac{G_1}{a_s^2\sqrt{1 - e_s^2}}\frac{h}{2m\mu}[-\hat{\mathbf{a}}\,\hat{\mathbf{p}}\cdot[\bar{\mathbf{B}}_1\sin(\Omega_{s_0}) + \bar{\mathbf{A}}_1\cos(\Omega_{s_0})] \\ & + 2\hat{\mathbf{a}}\,\hat{\mathbf{q}}\cdot[-\bar{\mathbf{A}}_1\sin(\Omega_{s_0}) + \bar{\mathbf{B}}_1\cos(\Omega_{s_0})] - \hat{\mathbf{b}}\,\hat{\mathbf{p}}\cdot[-\bar{\mathbf{A}}_1\sin(\Omega_{s_0}) \\ & + \bar{\mathbf{B}}_1\cos(\Omega_{s_0})] - 2\hat{\mathbf{b}}\,\hat{\mathbf{q}}\cdot[\bar{\mathbf{B}}_1\sin(\Omega_{s_0}) + \bar{\mathbf{A}}_1\cos(\Omega_{s_0})]]\end{aligned} \tag{72}$$

$$\begin{aligned}\dot{\bar{\mathbf{e}}} = {} & \frac{G_1}{a_s^2\sqrt{1 - e_s^2}}\frac{h}{2m\mu}[-\hat{\mathbf{a}}\,\hat{\mathbf{p}}\cdot[\bar{\mathbf{B}}_1\sin(\Omega_{s_0}) + \bar{\mathbf{A}}_1\cos(\Omega_{s_0})] \\ & + 2\hat{\mathbf{a}}\,\hat{\mathbf{q}}\cdot[-\bar{\mathbf{A}}_1\sin(\Omega_{s_0}) + \bar{\mathbf{B}}_1\cos(\Omega_{s_0})] - \hat{\mathbf{b}}\,\hat{\mathbf{p}}\cdot[-\bar{\mathbf{A}}_1\sin(\Omega_{s_0}) \\ & + \bar{\mathbf{B}}_1\cos(\Omega_{s_0})] - 2\hat{\mathbf{b}}\,\hat{\mathbf{q}}\cdot[\bar{\mathbf{B}}_1\sin(\Omega_{s_0}) + \bar{\mathbf{A}}_1\cos(\Omega_{s_0})]]\end{aligned} \tag{72}$$

where Ω_{s_0} is the location of the node of the heliocentric orbit in the rotating frame at periapsis. For a given Fourier coefficient C_i, the averaged value is

$$\bar{C}_i(j) = \frac{1}{2\pi}\int_0^{2\pi} \sin(n\lambda_v) C_i(j)\, \mathrm{d}\nu' \tag{73}$$

and the special case of the constant Fourier coefficient terms is

$$\bar{A}_0(j) = \frac{1}{2\pi}\int_0^{2\pi} A_0(j)\, \mathrm{d}\nu' \tag{74}$$

The Fourier coefficients vary over the orbit about the sun because different parts of the spacecraft are exposed to sunlight as it spins, or the same parts are exposed from different angles. These variations are often nonsmooth, due to the fact that new faces are being exposed or hidden. Therefore, the averaged Fourier coefficients generally need to be carried out numerically. Interestingly, if a satellite is considered where the orbit about Earth lies in the same plane as the Earth's orbit about the sun, the averaged Fourier coefficients would be exactly equal to the original values (ignoring Earth's shadow).

V. Satellite Application Example

A basic model based on the GRACE satellite was constructed as an extruded trapezoidal shape (Fig. 2) with size and radiative property data from the literature [3,14]. The body axes are aligned with the orbit at the start of the simulation as follows: $\hat{\mathbf{z}}_b$ is parallel with $\hat{\mathbf{h}}$, $\hat{\mathbf{x}}_b$ is parallel with $\hat{\mathbf{e}}$, and $\hat{\mathbf{y}}_b$ is parallel to $\hat{\mathbf{e}}_\perp$. As was stated earlier, the relationship with $\hat{\mathbf{z}}_b$ is fixed throughout the simulation, while the other two body axes rotate synchronously with the orbit. If $\hat{\mathbf{x}}_b$ and $\hat{\mathbf{y}}_b$ are not aligned correctly to start, the phase angle ϕ_0 is used to rotate the body to the correct orientation.

The radiative properties used are reproduced in Table 1. On the GRACE spacecraft, the top and sloped sides were solar panels, and thus they share the same optical properties. The same is true for the front and back of the spacecraft.

Following the methodology described by Scheeres [11] and the data from Table 1, the Fourier coefficients for this model were derived. The coefficients are plotted in Figs. 3–5. However, due to the symmetry of this shape, $\mathbf{A}_n(2)$, $\mathbf{B}_n(1)$, and $\mathbf{B}_n(3)$ are zero for all n and therefore are not plotted. The zenith angle is defined as the angle between $\hat{\mathbf{z}}_b$ and the spacecraft–sun unit vector. In each of these plots, all orders up to $n = 25$ are plotted; however, in most cases the magnitude falls off as n increases.

Several interesting relationships appear that are worth pointing out. First we note that $\mathbf{A}_0(2) = 0$. This means, by Eq. (46), that there is no secular growth in energy for a circular orbit with any zenith angle. Also, note that in Figs. 3–5 there is a kink in the coefficients near zenith angles of 50 and 130°. Between these zenith angles, both of the sloped sides of GRACE can see the sun, while outside those angles only one side is illuminated. Finally, it is interesting to note that all orders of the $\mathbf{A}_n(3)$ coefficients go to zero at a zenith angle of 90°. This will cause the secular rate for all components of the angular momentum vector to go to zero via Eq. (47) when the orbit is oriented in that manner.

Figures 3–5 show what can be considered the ideal values of the coefficients based on the available data before launch. However, the coefficients will almost certainly take on nonideal values, due to space weathering once the vehicle is on orbit. In particular, one can imagine the properties of the leading side ($+\hat{\mathbf{y}}_b$) to change differently from the trailing side. This would immediately impact the $\mathbf{A}_0(2)$ coefficient, which would then give rise to a secular change in energy.

Table 1 GRACE optical properties

Side	s	ρ
Front and back ($\pm\hat{\mathbf{y}}_b$)	0.4	0.26
Top and sides ($+\hat{\mathbf{x}}_b$, $\pm\hat{\mathbf{z}}_b$)	0.05	0.3
Bottom ($-\hat{\mathbf{x}}_b$)	0.68	0.2

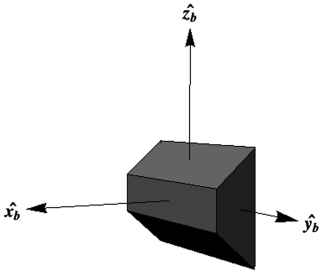

Fig. 2 Illustration of the GRACE model, with the body axes shown.

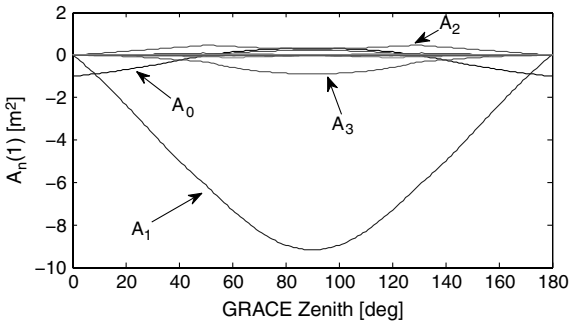

Fig. 3 $A_n(1)$ coefficient components. The most prominent orders are labeled.

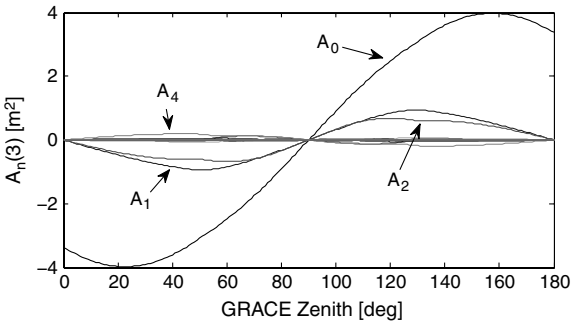

Fig. 4 $A_n(3)$ coefficient components. The most prominent orders are labeled.

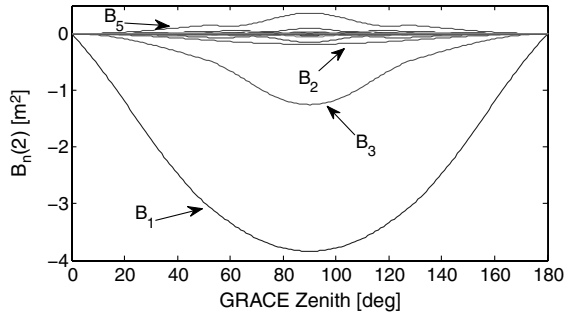

Fig. 5 $B_n(2)$ coefficient components. The most prominent orders are labeled.

This idea illustrates how the Fourier coefficients are observable to be estimated once the craft is launched.

These coefficients were used to model the perturbative effects on the orbit caused by the solar radiation. This simulation was run for 10 orbits and compares the numerical results with the secular results from the orbit averaging. This orbit is based on the nominal GRACE orbit and has an altitude of 500 km and an inclination of 90°. This simulation assumes that the sun is at a zenith angle of 60°.

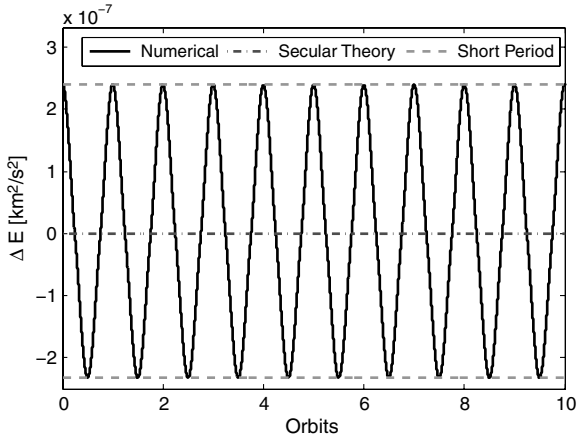

Fig. 6 Change in the orbital energy from its initial mean value over 10 orbits for the numerical integration and the orbit-averaged theory. The initial mean value is approximately $-28.98\ \mathrm{km^2/s^2}$. The dashed lines represent the bounds of the short-period variations as predicted by the theory in Sec. IV.C.

The results of this simulation are shown in Figs. 6–8. These plots compare a numerical integration of the equations of motion using a point-mass gravity model for Earth plus the full Fourier series up to $n = 25$ with the orbit-averaged theory described by Eqs. (46–48).

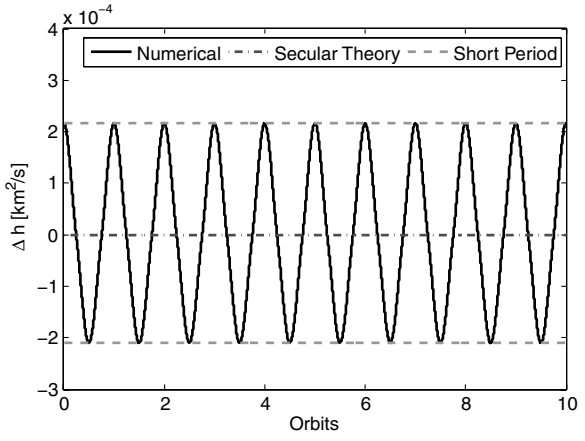

Fig. 7 Change in the orbital angular momentum magnitude from its initial mean value over 10 orbits for the numerical integration and the orbit-averaged theory. The initial mean value is approximately $52,360\ \mathrm{km^2/s}$. The dashed lines represent the bounds of the short-period variations as predicted by the theory in Sec. IV.C.

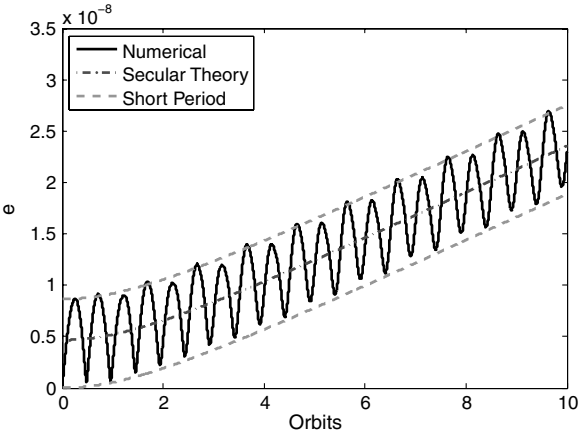

Fig. 8 Orbital eccentricity over 10 orbits for the numerical integration and the orbit-averaged theory. The dashed lines represent the bounds of the short-period variations as predicted by the theory in Sec. IV.C.

The secular theory includes the offsets from Eqs. (60–65), which is why the two simulations have a difference at the initial time. The secular theory does follow the average of the numerical integration closely. Also note that the predicted bounds of the short-period variations almost perfectly match those seen in the numerical simulation. The slight differences are due to the nonzero eccentricity that appears due to the secular variation, as well as higher-order drift that is not taken into account in our averaging methodology.

VI. Shadowing Analysis

The theory thus far has not accounted for the effect of the shadow from the primary body. When in the shadow, the sun is obscured from the view of the spacecraft [so that $P(R) = 0$], which results in the SRP force becoming zero while the spacecraft is in the shadow. When the orbit is orientated so that the spacecraft is passing through the shadow of the Earth, the Fourier coefficients used to describe the force will be different from those in Eq. (28).

To analyze the effects of the shadow on the orbit evolution, we create a *shadow force* to apply to the spacecraft when the orbit passes through the shadow. This shadow force is equal and opposite of the solar radiation force during the shadowing period and is zero elsewhere. By adding the original SRP model together with the shadow force model, the total effect will be to have the normal SRP acting on the satellite outside of the shadow, while having zero acceleration inside the shadow. Using this methodology has two benefits. First, the original set of Fourier coefficients, which are functions of the spacecraft's physical properties and attitude motion, are not modified. Second, the shadow force can be described by its own set of Fourier coefficients, which can then be used to determine how the presence of the eclipse changes to orbital effects of SRP.

A. Shadow Approach

The shadow force is defined as

$$\mathbf{F}_{\mathrm{sh}} = \begin{cases} 0 & 0 \le M < M_1 \\ -\mathbf{F}_{\mathrm{SRP}} & M_1 \le M \le M_2 \\ 0 & M_2 < M \le 2\pi \end{cases} \tag{75}$$

where M_1 is the mean anomaly at which the spacecraft enters the umbra, and M_2 is the mean anomaly where the spacecraft emerges from the umbra. The total force acting on the spacecraft due to SRP is now given by

$$\mathbf{F}_{\mathrm{tot}} = \mathbf{F}_{\mathrm{SRP}} + \mathbf{F}_{\mathrm{sh}} = \begin{cases} \mathbf{F}_{\mathrm{SRP}} & 0 \le M < M_1 \\ 0 & M_1 \le M \le M_2 \\ \mathbf{F}_{\mathrm{SRP}} & M_2 < M \le 2\pi \end{cases} \tag{76}$$

This is illustrated in Fig. 9.

The shadow force can be expressed as a new Fourier series in the mean anomaly as

$$\mathbf{F}_{\mathrm{sh}} = P(R) \sum_{n=0}^{\infty} [\mathbf{S}_n \cos(nM) + \mathbf{R}_n \sin(nM)] \tag{77}$$

where the coefficients can be derived as

$$S_0 = \frac{1}{2\pi} \int_{M_1}^{M_2} \frac{-\mathbf{F}_{\mathrm{SRP}}}{P(R)}\, \mathrm{d}M \tag{78}$$

$$S_n = \frac{1}{\pi} \int_{M_1}^{M_2} \frac{-\mathbf{F}_{\mathrm{SRP}}}{P(R)} \cos(nM)\, \mathrm{d}M \tag{79}$$

$$R_n = \frac{1}{\pi} \int_{M_1}^{M_2} \frac{-\mathbf{F}_{\mathrm{SRP}}}{P(R)} \sin(nM)\, \mathrm{d}M \tag{80}$$

for $n = 1, 2, \ldots, \infty$. The integration bounds can be changed from 0 and 2π, due to the fact that the shadow acceleration is zero outside of the umbra.

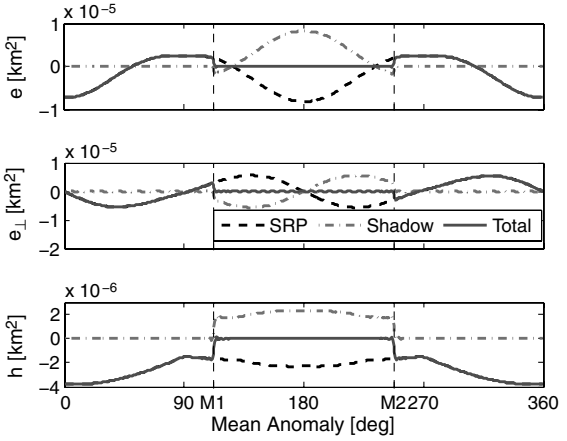

Fig. 9 Example of the effect of the Earth's shadow on GRACE in orbit frame coordinates. The shadow acceleration cancels out the original SRP acceleration for $M_1 \leq M \leq M_2$ so that the total acceleration is zero over this range. The mean anomaly is measured from the subsolar point on the orbit.

B. Orbital Effect of the Shadow

One of the main benefits of creating the shadow force is that we are able to decompose it into a Fourier series and then insert those coefficients directly into the equations for the orbital effects. The averaging theory we have applied to find the secular effects is a linear process; therefore, we are able to find the total average effects by adding the commensurate Fourier coefficients from the original SRP force and the shadow force in the secular results given in Eqs. (46–48). The total secular effects are

$$\bar{\dot{\mathcal{E}}} = \frac{P(R)}{m}\frac{h}{a}\hat{\mathbf{q}}\cdot(\mathbf{S}_0 + \mathbf{A}_0') \tag{81}$$

$$\bar{\dot{\mathbf{h}}} = \frac{P(R)}{m}\frac{a}{2}[\hat{\mathbf{a}}\,\hat{\mathbf{h}}\cdot(\mathbf{R}_1 + \mathbf{B}_1') - \hat{\mathbf{b}}\,\hat{\mathbf{h}}\cdot(\mathbf{S}_1 + \mathbf{A}_1') + 2\hat{\mathbf{h}}\,\hat{\mathbf{q}}\cdot(\mathbf{S}_0 + \mathbf{A}_0')] \tag{82}$$

$$\bar{\dot{\mathbf{e}}} = \frac{P(R)}{m}\frac{h}{2\mu}[\hat{\mathbf{a}}\,\hat{\mathbf{p}}\cdot(\mathbf{R}_1 + \mathbf{B}_1') + 2\hat{\mathbf{a}}\,\hat{\mathbf{q}}\cdot(\mathbf{S}_1 + \mathbf{A}_1') - \hat{\mathbf{b}}\,\hat{\mathbf{p}}\cdot(\mathbf{S}_1 + \mathbf{A}_1') + 2\hat{\mathbf{b}}\,\hat{\mathbf{q}}\cdot(\mathbf{R}_1 + \mathbf{B}_1')] \tag{83}$$

While these expressions have the same form as the original expressions, they are not as simple. In the nonshadow case, only seven coefficients are required to describe the secular effects. The shadow coefficients are technically functions of all of the original Fourier coefficients, however, and therefore the secular results now effectively depend on all of the Fourier coefficients.

The shadow coefficients can also be used to describe the short-term dynamics. For example, using Eq. (57), the short-term dynamics for the energy evolution are now described as

$$\bar{\mathcal{E}}_p = \frac{P(R)}{m}\frac{h}{a}\sqrt{\frac{a^3}{\mu}}\hat{\mathbf{q}}\cdot\frac{1}{2\pi}\int_0^{2\pi}\Bigg\{(\mathbf{S}_0 + \mathbf{A}_0')\cdot(M - M_0) + \sum_{n=1}^{\infty}\frac{1}{n}[(\mathbf{S}_n + \mathbf{A}_n')\sin(nM) - (\mathbf{R}_n + \mathbf{B}_n')\cos(nM) - (\mathbf{S}_n + \mathbf{A}_n')\sin(nM_0) + (\mathbf{R}_n + \mathbf{B}_n')\cos(nM_0)]\Bigg\}\,\mathrm{d}M - \pi\sqrt{\frac{a^3}{\mu}}\bar{\mathcal{E}}(\mathbf{x}_0) \tag{84}$$

where $\bar{\mathcal{E}}(\mathbf{x}_0)$ is determined from Eq. (81).

The shadow of the planet will change the secular rates and the short-period dynamics of the satellite. The total effect the shadow is dependent on many factors: most notably, the shape and optical properties of the satellite, for what part of the orbit the satellite is obscured and for how long.

C. Penumbra Models

The theory so far has not included a penumbra; however, this can be added easily in the same manner. There are two models of interest for the penumbra. The first is the most simple model, which decreases the solar radiation force in proportion of the amount of the solar disk that is occluded by the solid Earth. The second, more accurate, model, which was developed by Vokrouhlicky et al. [15], models the effect of the Earth's atmosphere in decreasing the solar radiation pressure, as well as the classical penumbra caused by the solid Earth.

No matter which form for the penumbra model is used, the shadow acceleration will be changed slightly to be derived as follows. The piecewise function will now be

$$\mathbf{F}_{\text{sh}} = \begin{cases} 0 & 0 \leq M < M_{p1} \\ -C_{\text{pen}}(M)\mathbf{F}_{\text{SRP}} & M_{p1} \leq M \leq M_1 \\ -\mathbf{F}_{\text{SRP}} & M_1 \leq M \leq M_2 \\ -C_{\text{pen}}(M)\mathbf{F}_{\text{SRP}} & M_2 \leq M \leq M_{p2} \\ 0 & M_{p2} < M \leq 2\pi \end{cases} \tag{85}$$

where M_{p1} is the mean anomaly at which the penumbra begins, M_{p2} is the mean anomaly where the penumbra ends, and $C_{\text{pen}}(M)$ is the scale factor for the penumbra model, which depends on the mean anomaly. In this case, the shadow acceleration coefficients are determined by adding the integral of each of the three parts of the above piecewise function.

In the preliminary testing, the penumbra impact is insignificant on the secular rates, assuming that the penumbra ($\Delta M \sim 0.5°$) is small compared to the umbra ($\Delta M \sim 40°$) and that it is symmetric about the umbra. However, if the penumbra is nonsymmetric, meaning that the penumbra on one side of the umbra is bigger than the other side for the same orbit, there can be arbitrarily large changes in the secular rates, including sign changes. However, whether this is physically possible or not is beyond the scope of this paper. Future investigations applying the shadowing theory to the GRACE example will help to quantify the realistic effects.

VII. Navigation Applications

The main goal of using the Fourier series model for spacecraft is the benefits it can give for navigation and orbit determination purposes. Estimation with our model does not attempt to determine the values of surface optical properties. Rather, we only estimate the Fourier coefficients that describe the effect of SRP on the orbit. This allows for the possibility of independently estimating the Fourier coefficients that affect the orbit in different ways, instead of having to estimate one scale factor that would change all of the Fourier coefficients.

The first step in applying estimation theory to our model is to conduct a sensitivity/covariance study of coefficients. The effects of the Fourier coefficients are nearly linearly independent, and therefore each can be estimated in turn. This can be clearly demonstrated by looking at Eqs. (46–48). Taking the partial of each of these equations in turn with respect to each of the seven Fourier coefficients present shows that there is no linear dependence in energy or the angular momentum vector components. The eccentricity does have two components acting in each direction. However, these coefficients only appear here, not in energy or angular momentum. Therefore, the linear dependence does not matter for a secular prediction, and the coefficients could be lumped if no accelerometer information is available to separate them. Given that the coefficients appear independently, it will be beneficial to go forward with a sensitivity study to quantify how accurately each coefficient should be estimated for use in the orbit determination problem.

There are several different methods we can use with this theory to estimate values for the coefficients. First, the secular results, Eqs. (46–48), can be used to estimate the low-order coefficients based on the average change in the orbital elements. This is a unique application of our theory that is not available with other current SRP

models. Second, a fast Fourier transform can be performed on accelerometer data over an orbit to get an estimate of all orders of coefficients in the body frame [see Eq. (17)], as this is exactly how a Fourier series would be determined from this data. Each of the Fourier coefficients is linearly independent over the mean anomaly by definition, and therefore this method could be used to separately estimate the coefficients when needed, especially in the case of the eccentricity effects as mentioned above. Finally, the presence of a shadow on an orbit can give us valuable information about the coefficients. When no shadow is present, only seven of the most significant coefficients affect the secular change in the orbit. However, when a shadow is present, all coefficients have some input into the secular rates through the shadow acceleration series [see Eqs. (81–83)]. This information can be used to separate the effects of the different coefficients.

In reality, the effects of SRP on the orbit are correlated with the effects of the other forces acting on the spacecraft. The particular method of dealing with this in terms of estimating the Fourier coefficients will depend on the orbit determination process being used for the particular mission. If the goal of the orbit determination process is purely to get the best fit of the orbit, then using a method such as estimating small time-varying stochastic accelerations to account for mismodeling of dynamics instead of estimating the Fourier coefficients, as is done for the Jet Propulsion Laboratory's (JPL's) International GNSS (Global Navigation Satellite System) Service orbit determination for GPS [16]. On the other hand, if estimating the solar radiation pressure itself is useful, such as in the GRACE mission [3], then a determination of what Fourier coefficients to estimate and their relationship to the other force models (e.g., Earth albedo, thermal radiation) in the orbit determination process will need to be explored.

As an early indication of the usefulness of our equations in the orbit determination problem, it is instructive to investigate the models used for GPS orbit estimation. The models created at The Aerospace Corporation [12], JPL [9], and Bern University [8], which have been used to varying degrees of success [17], have been based on differently parametrized Fourier series. Given the similarity of these models, particularly between the Bern and JPL models, let us examine the Bern model for comparison. The main point to make in comparison with our equations is that the Bern model is a truncated Fourier series based on the location of the sun compared to the satellite in its orbit. The Bern model equations are included in the Appendix for comparison. In effect, the model is parametrized similarly to our model based on the faster orbit variation and the slower year variation. In the Bern model, the difference between the argument of latitude for the satellite and the sun represents the orbit variation, and the elevation angle of the sun from the orbit plane represents the yearly variation. These compare almost directly to our use of the solar longitude λ_s and latitude δ_s in the rotating frame. Over each orbit, the Bern model contains constant terms, terms that vary once per orbit, and one term that varies 3 times per orbit. It can be immediately stated from our results that the term that varies 3 times per orbit will have no effect on the secular change of the orbit, although it may influence the short-period variations. Also, only the constant terms in the velocity direction have an impact on the secular change in the orbit. It would appear that our model offers good insight into the effects of SRP on the GPS orbit that is not immediately apparent from the Bern model. On the other hand, the derivation in this paper helps to justify why the Bern model can successfully model the SRP acceleration for orbit determination.

It is worth taking a moment here to more closely consider the cannonball model from the Appendix, which was used for LAGEOS [1] as well as many other applications. If this model were made into a Fourier series in the rotating frame, the only nonzero coefficients would be $\mathbf{A}_1(1)$, $\mathbf{B}_1(2)$, and possibly $\mathbf{A}_0(3)$, depending on the solar latitude. In fact, in this model the coefficients would also be subject to the constraint that $\mathbf{A}_1(1) = \mathbf{B}_1(2)$, because the acceleration is assumed to be of constant magnitude. The effect of this model, as seen from Eqs. (46–48), is that only the eccentricity vector will change in a secular manner, due to the solar radiation pressure (for nonzero eccentricities the angular momentum will also vary [10]). This is fine, as long as the surface of the spacecraft is perfectly uniform optically and a perfectly uniform shape. However, as soon as the surface undergoes any weathering on orbit, many other Fourier coefficients will take on nonzero values, which will change the orbit evolution, possibly dramatically.

Finally, it is mentioned again that the general equations for elliptical orbits have been developed [10]. While these equations are not as simple as the circular results, they do give us a similar form that should allow for good estimation of the coefficients and therefore the same benefits as we discuss here. Furthermore, the general equations were also expressed as series in eccentricity, so for orbits with small but finite values of eccentricity, the secular rates can still be expressed as functions of a small number of Fourier coefficients.

There is a large amount of future work for this topic. The theory will be extended in several ways. First, we will apply the theory to another spacecraft (such as GPS) to show that it is applicable when the attitude motion is more complicated than with a spacecraft like GRACE. Next, we will fully develop and apply the method for handling the Earth's shadow. Another extension will include testing what will happen when the rotation is not purely synchronous. Finally, we will be investigating different methods for estimating the Fourier coefficients from observation data in order to make this model useable for the orbit determination problem.

VIII. Conclusions

This paper presents a new force model for the solar radiation pressure acting on a spacecraft in Earth orbit. This model assumes that the spacecraft has a nominal attitude motion that repeats with the orbit. In this case, the SRP force can be mapped to a frame that rotates uniformly with the mean motion of the orbit. The force is expressed as Fourier series with respect to the mean anomaly, where the coefficients may themselves vary over the course of the year, depending on the geometry of the orbit. The variational equations for the orbit were derived with respect to this force model, and the secular term and short-period dynamics were derived in terms of the Fourier coefficients. The theory was extended to account for cases when the spacecraft passes through the Earth's orbit, which can be done through a systematic modification of the Fourier coefficients. It was shown that for a satellite in a circular orbit, the secular effects of solar radiation pressure can be fully described with only seven Fourier coefficients. A specific example based on the GRACE satellite was shown to illustrate the theory presented.

The appeal of this theory is that it brings together the methods of SRP force modeling based on the body models and physical parameters with methods for analyzing the orbital effects due to perturbative forces. This allows for a priori values to be found for a Fourier series model that is very similar to those that have been used successfully for precise orbit determination of the GPS satellites. This paper presented a theory to apply a similar methodology to many Earth orbiters, in hopes of improving their mission design and orbit determination accuracy.

Appendix: Previous SRP Models

The LAGEOS, or cannonball model [1], is based on the spacecraft being a simple sphere with all incident radiation being reflected directly back at the sun. It is written as

$$\mathbf{a}_{\text{SRP}} = C_R \frac{P(R)}{m} A \hat{\mathbf{u}} \tag{A1}$$

The GRACE model [3] looks more like Eq. (15). The spacecraft is represented by the six major surfaces, with each surface having its own optical properties. This model is written as

$$\mathbf{a}_{\text{SRP}} = -C_R \frac{P(R)}{m} \sum_{k=1}^{6} A_k \cos\theta_k \left[(1 - s_k)\hat{\mathbf{u}} + 2\left(\frac{\rho_k}{3} + s_k \cos\theta_k\right)\hat{\mathbf{n}}_k \right] \tag{A2}$$

where k is the index for each surface of the satellite. Each surface has a normal unit vector $\hat{\mathbf{n}}_k$, a surface area A_k, and specular and diffuse reflectivity coefficientss_k and ρ_k, respectively. Finally, $\cos\theta_k = \hat{\mathbf{u}} \cdot \hat{\mathbf{n}}_k$ and θ_k is the angle between the two unit vectors of interest.

Note that both of these models use a scalar adjustment coefficient C_R to modify the resultant acceleration as necessary.

The Bern model [8] is used to estimate the solar radiation pressure acting on GPS satellites. The SRP caused acceleration is assumed to have the form

$$\mathbf{a}_{\text{SRP}} = D(\beta_0)\hat{\mathbf{e}}_D + Y(\beta_0)\hat{\mathbf{e}}_Y + B(\beta_0)\hat{\mathbf{e}}_B + Z_1(\beta_0)\sin(u-u_0)\hat{\mathbf{e}}_Z + [X_1(\beta_0)\sin(u-u_0) + X_3(\beta_0)\sin(3u-u_0)]\hat{\mathbf{e}}_X \quad \text{(A3)}$$

where $\{\hat{\mathbf{e}}_D, \hat{\mathbf{e}}_Y, \hat{\mathbf{e}}_B\}$ are body-fixed frame unit vectors, $\hat{\mathbf{e}}_Z = \hat{\mathbf{h}}$, $\hat{\mathbf{e}}_X = -\hat{\mathbf{p}}$, β_0 is the elevation of the sun above the orbital plane, u is the satellite's argument of latitude, and u_0 is the argument of latitude of the sun position projected onto the orbital plane. Each of the coefficients (D, Y, B, X_1, X_3, and Z_1) are a function of constant terms plus periodic terms based on β_0.

Acknowledgments

The authors would like to acknowledge the support for this research provided by grant NNX08AL51G from NASA's Planetary Geology and Geophysics program. We would also like to thank the reviewers for their insightful comments.

References

[1] Lucchesi, D. M., "Reassessment of the Error Modelling of Nongravitational Perturbations on LAGEOS II and Their Impact in the Lense-Thirring Determination. Part I," *Planetary and Space Science*, Vol. 49, 2001, pp. 447–463. doi:10.1016/S0032-0633(00)00168-9

[2] Marshall, J. A., and Luthcke, S. B., "Modeling Radiation Forces Acting on TOPEX/Poseidon for Precision Orbit Determination," *Journal of Spacecraft and Rockets*, Vol. 31, No. 1, Jan.–Feb. 1994, pp. 99–105. doi:10.2514/3.26408

[3] Cheng, M., Ries, J. C., and Tapley, B. D., "Assessment of the Solar Radiation Model for GRACE Orbit Determination," *Advances in the Astronautical Sciences*, Vol. 129, 2008, pp. 501–510.

[4] Ziebart, M., "Generalized Analytical Solar Radiation Pressure Modeling Algorithm for Spacecraft of Complex Shape," *Journal of Spacecraft and Rockets*, Vol. 41, No. 5, Sept.–Oct. 2004, pp. 840–848. doi:10.2514/1.13097

[5] Rim, H.-J., Webb, C. E., Yoon, S., and Schutz, B. E."Radiation Pressure Modeling for ICESat Precision Orbit Determination," AIAA/AAS Astrodynamics Specialist Conference and Exhibit, AIAA Paper 2006-6666, Keystone, CO, Aug. 2006.

[6] Fritsche, B., and Klinkrad, H., "Accurate Prediction of Non-Gravitational Forces for Precise Orbit Determination. Part I: Principles of the Computation of Coefficients of Force and Torque," AIAA/AAS Astrodynamics Specialist Conference and Exhibit, AIAA Paper 2004-5461, Providence, RI, Aug. 2004.

[7] Doornbos, E., "Modeling of nongravitational forces for ERS-2 and ENVISAT," M.S. Thesis, Delft Inst. for Earth-Oriented Space Research, Delft Univ. of Technology, Delft, The Netherlands, July 2001.

[8] Springer, T., Beutler, G., and Rothacher, M., "A New Solar Radiation Pressure Model for GPS Satellites," *GPS Solutions*, Vol. 2, No. 3, 1999, pp. 50–62. doi:10.1007/PL00012757

[9] Bar-Sever, Y. E., "New and Improved Solar Radiation Pressure Models for GPS Satellites Based on Flight Data," Jet Propulsion Lab., Pasadena, CA, 1997.

[10] McMahon, J., and Scheeres, D., "Secular Orbit Variation Due to Solar Radiation Effects: A Detailed Model for BYORP," *Celestial Mechanics and Dynamical Astronomy*, Vol. 106, 2010, pp. 261–300. doi:10.1007/s10569-009-9247-9

[11] Scheeres, D. J., "The Dynamical Evolution of Uniformly Rotating Asteroids Subject to YORP," *Icarus*, Vol. 188, 2007, pp. 430–450. doi:10.1016/j.icarus.2006.12.015

[12] Fliegel, H. F., and Gallini, T. E., "Solar Force Modeling of Block IIR Global Positioning System Satellites," *Journal of Spacecraft and Rockets*, Vol. 33, No. 6, Nov.–Dec. 1996, pp. 863–866. doi:10.2514/3.26851

[13] Hudson, J., and Scheeres, D. J., "Reduction of Low-Thrust Continuous Controls for Trajectory Dynamics," *Journal of Guidance, Control, and Dynamics*, Vol. 32, May–June 2009, pp. 780–787. doi:10.2514/1.40619

[14] Bettadpur, S., "GRACE: Product Specification Document," Center for Space Research, Univ. of Texas at Austin, Rept. GRACE 327-720, Austin, TX, 2007.

[15] Vokrouhlicky, D., Farinella, P., and Mignard, F., "Solar Radiation Pressure Perturbations for Earth Satellites. Part I: A Complete Theory Including Penumbra Transitions," *Astronomy and Astrophysics*, Vol. 280, 1993, pp. 295–312.

[16] Bar-Sever, Y. E., and Kuang, D., "New Empirically Derived Solar Radiation Pressure Model for Global Positioning System Satellites," *The Interplanetary Network Progress Report*, Vol. 42, No. 159, Nov. 2004, pp. 1–11.

[17] Chen, J., and Wang, J., "Models of Solar Radiation Pressure in the Orbit Determination of GPS Satellites," *Chinese Astronomy and Astrophysics*, Vol. 31, 2007, pp. 66–75. doi:10.1016/j.chinastron.2007.01.002